12th IFAC International Symposium on
Advanced Control of Chemical Processes
July 14-17, 2024. Toronto, Canada

Monitoring of product temperature and cycle duration in multi-vial lyophilization

A. Chia * **J. Bouchard** ** **É. Poulin** ***

* *Department of Electrical and Computer Engineering, LOOP, Université Laval, Quebec City, QC, Canada (e-mail: lydia-andrea.gonzalez-chia@ulaval.ca).*
** *Department of Chemical Engineering, LOOP, Université Laval, Quebec City, QC, Canada (e-mail: jocelyn.bouchard@gch.ulaval.ca)*
*** *Department of Electrical and Computer Engineering, LOOP, Université Laval, Quebec City, QC, Canada (e-mail: eric.poulin@gel.ulaval.ca)*

Abstract: The implementation of an in-line control strategy for primary drying relies on the availability of the product temperature and sublimation front position. Such measurements are often inaccessible or difficult to obtain directly without interfering with the drying trajectory, thus motivating the design of in-line estimators. This article specifically addresses this issue, taking advantage of a global mass loss measurement and spatial characterization of vials along the chamber. The estimator proposed uses a least square algorithm and simplified models to re-calibrate the heat transfer coefficient related to different vial locations. Results allow comparing the quality of the estimations with regard to the product temperature and cycle time predictions under parametric disturbances and plant/model mismatch.

Keywords: Lyophilization, freeze-drying, primary drying, sublimation flux, variable estimation, nonlinear least-square.

1. INTRODUCTION

Lyophilization is a drying technique largely used in the pharmaceutical industry to preserve and stabilize chemically reactive and temperature-sensitive products. The main stages involved are freezing, primary drying, and secondary drying. Among them, primary drying is the longest and represents between 67% to 69% of the overall electric consumption of pilot and industrial units (Stratta et al., 2020). Implementing a control strategy for primary drying relies on the availability of measurements for key process variables, such as the product temperature, sublimation flux, and primary drying endpoint. A batch comprises hundreds or thousands of vials, and determining the drying trajectories of multiple vials can be challenging because of the different dynamics exhibited by vials at specific locations on the equipment. Currently available instrumentation shows limited sensor precision, and restricted applicability in production-scale equipment. In particular for key local variables such as the sublimation front position and product temperature. In-line estimators have been considered to remedy this issue.

An estimator associates knowledge of the physical system (model) and available measurements to estimate the unknown or poorly measured parameters and process variables. Most of the applications published on the subject rely on product temperature measurement using thermocouples (Velardi et al., 2009, 2010; Bosca et al., 2017; Fissore et al., 2017). Drawbacks come from the intrusiveness, sensor misplacement, and the potential bias impacting the drying dynamics of monitored vials. Furthermore, thermocouples are often unsuitable for production-scale applications due to sterility problems and because the probe insertion is not feasible in equipment with an automated vial loading/unloading system. Other estimation approaches using global measurements, such as the pressure rise test (PRT) (Fissore et al., 2010), close the valve between the drying chamber and condenser for a short period (typically 30 s), and calculate the average product temperature from the pressure rise profile. The accuracy of the estimations depends on processing conditions, high rate sublimation being particularly challenging (Pisano et al., 2017). Furthermore, most PRT-based algorithms used to estimate the product temperature are only reliable in the first part of a primary drying cycle (Barresi et al., 2010). Spectroscopy analyzers, like the tunable diode laser absorption spectroscopy (TDLAS), give the global flowrate of water vapor, which, along with a heat transfer coefficient, can be transformed into an average product temperature (Sharma et al., 2019). However, approaches based on PRT and TDLAS provide an average temperature value that is mostly related to that of center vials but is not representative of the batch (due to heterogeneity).

A practical approach for estimators should use non-invasive instrumentation, with applicability to both pilot and industrial scale equipment, and incorporate drying heterogeneity in the design. This work introduces an in-line estimator for the primary drying stage of pharmaceutical lyophilization in multiple vials. It takes advantage of a global measurement of the sublimed water vapor

and a phenomenological model. A nominal heat transfer coefficient, from which different heat contributions can be derived along the shelf accounts for intra-lot heterogeneity. The estimator is evaluated in simulation using the case study of a previously characterized product (Chia et al., 2022). The performance comparison with an open-loop observer assesses the quality of the predictions with respect to product temperature and drying time under parametric and external disturbances. This paper is structured as follows. Section 2 details a set of fundamental equations for primary drying. Then, section 3 illustrates the design of the in-line estimator, which is evaluated through simulation in section 4.

2. PROCESS MODEL

Pikal (1985) describes primary drying for a single vial using a set of algebraic-differential equations with two inputs, the chamber pressure P and shelf temperature T_s, and three outputs, the temperature of the product at the bottom of the vial T_B, sublimation flux of water vapor N_w, and rate of change of the sublimation front $\dot{h}$. The model has been experimentally validated and widely used in literature for process optimization (Chia et al., 2023). It distinguishes two regions: a frozen matrix of the sample solution and a dry layer that begins to form as sublimation occurs. A moving interface, called the sublimation front position h, separates these two regions. The model assumes that heat is supplied only at the bottom of the vial and is used solely for sublimation (neglecting the effect of heat accumulation). Also, the sublimation interface is considered to be planar and parallel to the vial bottom, and only water vapor constitutes the gas phase within the dried layer.

The mass balance in the frozen layer yields the evolution of the sublimation front through

$$\dot{h} = -\frac{1}{\rho_f - \rho_d} N_w \tag{1}$$

where ρ_f and ρ_d are the density of the frozen and dried layer, respectively. N_w is the sublimation flux calculated as

$$N_w = \frac{1}{R_p}[P_w - P] \tag{2}$$

where R_p is the resistance of the dried layer to vapor flow, and P_w the water vapor saturation pressure related to the temperature of the interface through

$$P_w = 133.3224 \left(2.69\text{E}10 \exp\left(\frac{-6144.96}{T_i}\right)\right) \tag{3}$$

The temperature of the product at the sublimation front is expressed as

$$T_i = T_s - \frac{\Delta H_s}{R_p}[P_w - P]\left(\frac{1}{K_v} + \frac{h}{\lambda_f}\right) \tag{4}$$

where K_v is the heat transfer coefficient, ΔH_s is the heat of sublimation of ice, and λ_f is the thermal conductivity of the frozen cake. The resolution of (1 – 4) yields the position and temperature of the sublimation front. Lastly,

$$T_B = T_s - \frac{1}{K_v}\left(\frac{1}{K_v} + \frac{h}{\lambda_f}\right)^{-1}[T_s - T_i] \tag{5}$$

provides the temperature of the product at the bottom of the vial.

Two parameters require experimental calibration: the heat transfer coefficient K_v, and dried layer resistance R_p. The former captures the various heat contributions not considered in the model assumptions, namely, convective heat between the shelf and vial bottom, and radiative heat from shelves, surrounding vials, and chamber walls. K_v is a function of the vial geometry and position in the chamber, as well as the chamber pressure P. The relation between K_v and P is expressed through the following equation (Pikal et al., 1984)

$$K_v = k_1 + \frac{k_2 P}{1 + k_3 P} \tag{6}$$

where k_1, k_2 and k_3 are empirical parameters. k_2 and k_3 express the dependency of K_v with P and the vial geometry, while k_1 accounts for the vial position on the shelf. If the pressure remains constant during the cycle, K_v becomes a constant. However, due to the different heat contributions, the same value would not be used for every vial on the shelf. The resistance of the dried layer to mass flux is affected by the sample formulation and thickness, stopper, vial geometry, and freezing protocol. It is proportional to the dried layer thickness $(L - h)$, thus increasing as sublimation occurs. The following empirical equation (Pikal et al., 1984)

$$R_p = k_4 + \frac{k_5(L - h)}{1 + k_6(L - h)} \tag{7}$$

where k_4, k_5 and k_6 are empirical parameters, relates R_p to $(L - h)$.

In practice, vials within the same batch exhibit various drying trajectories (caused by the different heat contributions) depending on their location. While conduction from the shelf is the primary source of heat to the vial, radiation and convection can have a large impact on the non-uniformity of the drying evolution (Pikal, 2000). Radiant heat comprises the contributions of the chamber door, walls, and the shelves above the vials. Those at the center of the shelf (surrounded by other vials) exhibit a minimum radiation effect, while those at the edges exhibit faster drying rates and higher product temperatures.

This study models the intra-lot heterogeneity using a nominal heat transfer coefficient, from which individual heat contributions can be derived relatively, hence creating a spatial distribution of K_v along the shelf. The value of K_v for a given position remains constant during a primary drying cycle. Previous studies have used a heterogeneity ratio to relate the heat contributions between center and edge vials (Rajniak et al., 2022). Furthermore, Pikal et al. (2016) claims that the calibration for edge vials extrapolates well from laboratory to industrial scale equipment in normal operating conditions.

In order to fit model predictions with experimental data, the global flowrate of water vapour $\dot{m}_{\mathrm{H_2O}}$ is the sum of the individual sublimation flux value of every vial in the chamber

$$\dot{m}_{\mathrm{H_2O}} = \sum_{i=1}^{n} N_{w,i} A_p \tag{8}$$

where n is the number of vials, A_p is the cross-sectional area of a vial, and $N_{w,i}$ are the calibrated model predictions of the sublimation flux of each vial.

3. IN-LINE ESTIMATION

This study uses the global sublimation flow rate of water vapor as an indicator of batch dynamics. The design of an in-line estimator requires a measurement acquired using sensors commonly found in pilot and industrial equipment, or that can be installed without major modifications and avoiding intrusiveness. As a solution to the instrumentation issues mentioned in Section 1, Pisano et al. (2014) introduced the pressure decrease test as an alternative measurement technique. It consists of closing the leakage valve that provides the inert gas to the drying chamber and analyse the response to provide an estimation of the global flow rate of water vapor. In this case, the procedure momentarily decreases the chamber pressure and product temperature. A non-invasive option to the PDT that uses a similar principle is the valveless monitoring system (VMS) (Fissore et al., 2015; Pisano et al., 2016). It relates the pressure difference between the chamber and condenser to the global sublimation flow rate of water vapor. This method requires a prior calibration of the equipment to relate the flow rate and pressure drop, a flowmeter for the inert gas injection, and two capacitance sensors to measure the differential pressure between the chamber and condenser. Among the above-mentioned techniques, the non-invasive VMS approach provides an indirect measurement of $\dot{m}_{\mathrm{H_2O}}$ using sensors typically available in pilot and production units.

Providing that it is possible to obtain a measurement of the sublimation flow rate using non-invasive instrumentation, the next step is the design of an estimator based on this measurement. The objective is to predict the product temperature of different vials and the drying time of the batch, using only the measurements of the shelf temperature, chamber pressure, and global flow rate of water vapor. Figure 1 provides the structure of the estimator. First, an optimization problem is solved using a nonlinear least square algorithm (NLS) and the available measurements are used to re-calibrate the nominal heat transfer coefficient. Then, the obtained values are inputted into the phenomenological models to predict the targeted process variables for individual vials. At every discrete time k, the

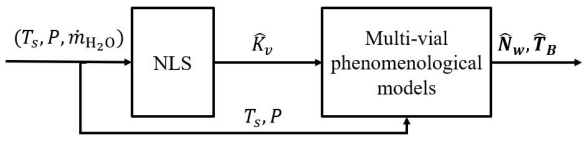

Fig. 1. Schematic of the in-line estimator.

workflow consists of solving

$$\hat{K}_v = \arg\min J \tag{9}$$

where

Table 1. Glycine properties and vial geometry.

Name	Value	Units
A_p	1.13 E − 4	m^2
A_v	1.77 E − 4	m^2
ΔH_s	2.69 E6	J/kg
λ_f	2.56	W/m K
ρ_f	918	kg / m^3
ρ_d	250	kg / m^3
L	9 E − 3	m
V	1 E − 6	m^3
T_c	269	K

$$J = \frac{1}{\mathcal{N}} \sum_{i=0}^{\mathcal{N}-1} (\dot{m}_{\mathrm{H_2O}}(k-i) - \hat{\dot{m}}_{\mathrm{H_2O}}(k-i))^2 + \Lambda \left(\frac{1}{\mathcal{N}} \sum_{i=0}^{\mathcal{N}-1} (K_v(k-i) - \hat{K}_v(k-i))^2 \right) \tag{10}$$

where $\mathcal{N}$ is the estimation window, K_v is the nominal value from prior calibration, and Λ is a weight to penalize the deviation between nominal and estimated K_v. If Λ is set to zero, the criteria will freely adjust K_v based only on the readings of $\dot{m}_{\mathrm{H_2O}}$. This could be problematic in the case of strongly biased measurements. $\dot{m}_{\mathrm{H_2}O}$ comes from the experimental data and $\hat{\dot{m}}_{\mathrm{H_2O}}$ is predicted from the process model in (8). The process model applies the phenomenological equations (1 - 5) inputted with the measured P and T_s, the nominal R_p, and $\hat{K}_v$. Note that these equations are only valid for vials where sublimation is ongoing, that is when the sublimation front is $0 < h \leq L$.

At the beginning of the simulation, the window size equals the number of samples, and after the first $\mathcal{N}$ samples, the window starts moving with a truncated size of $\mathcal{N}$. After the optimization problem provides the optimal K_v that minimizes J in (9), this nominal value is used to derive the heat contributions in different vial positions and therefore predict the individual values of N_w and T_B using equations (1 - 5).

4. RESULTS AND DISCUSSION

4.1 Case study

The case study selected to illustrate the in-line estimator is the lyophilization of a 5% w/w solution of glycine from Bio Basic Inc and distilled water (Chia et al., 2022). A total of 20 vials with 3.7 ml capacity were filled with 1 ml of the formulation, Table 1 summarizes the product properties and vial geometry.

Vial distribution in Figure 2 illustrate the heat contributions of different vials within the batch. There are three zones, and the heat transfer in each one of them correspond to: K_v for zone *I*, 1.5 K_v for zone *II* and 2.2 K_v for zone *III*. The nominal K_v was experimentally calibrated and is computed using (6) with the coefficients presented in Table 2.

To display the difference in the evolution of the drying dynamics for the vial zones in this case study, Figure 3 shows the prediction of a drying cycle using the phenomenological models and considering standard operating conditions.

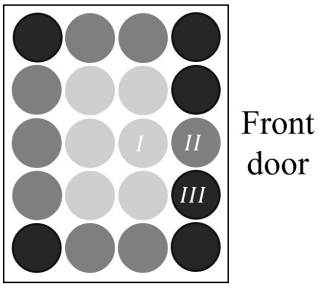

Fig. 2. Spatial variation of the heat contributions in the shelf.

Table 2. Heat transfer coefficients for nominal K_v.

Name	Value	Units
k_1	12.34	J/m^{2}s K
k_2	1.62	J/m^{2}s K Pa
k_3	0.33	1/Pa

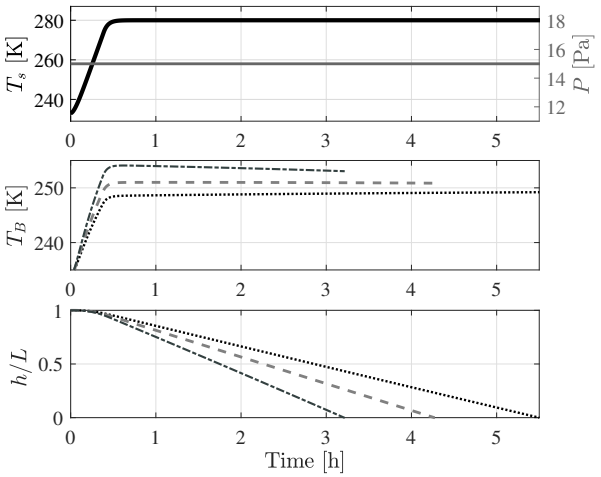

Fig. 3. Performance of the vial zones considering standard profiles for T_s and P. Shelf temperature (—) and chamber pressure (—), along with model predictions of T_B and h/L for vials of zone I (••), zone II (– –), and zone III (–•).

In this cycle, the chamber pressure is set constant at 15 Pa, and the shelf temperature increases from 233 K to 280 K at a rate of 1 K/min. The vials in zone III, with a higher heat transfer coefficient, exhibit a higher product temperature and sublimation flux. Which in turn leads to a faster drying time of around 3.4 h when compared to the 5.3 h for vials of zone I. Note that in multi-vial primary drying, the cycle time of the batch corresponds to the drying duration of the vials with the slowest dynamics. In this case, the duration is determined by the cycle time of vials in zone I.

4.2 Estimation results

Numerical validation is carried out using the phenomenological model to simulate the primary drying of the batch of 20 vials, characterized by the different values of heat transfer coefficient. An open-loop estimator provides the baseline performance comparison in each simulation

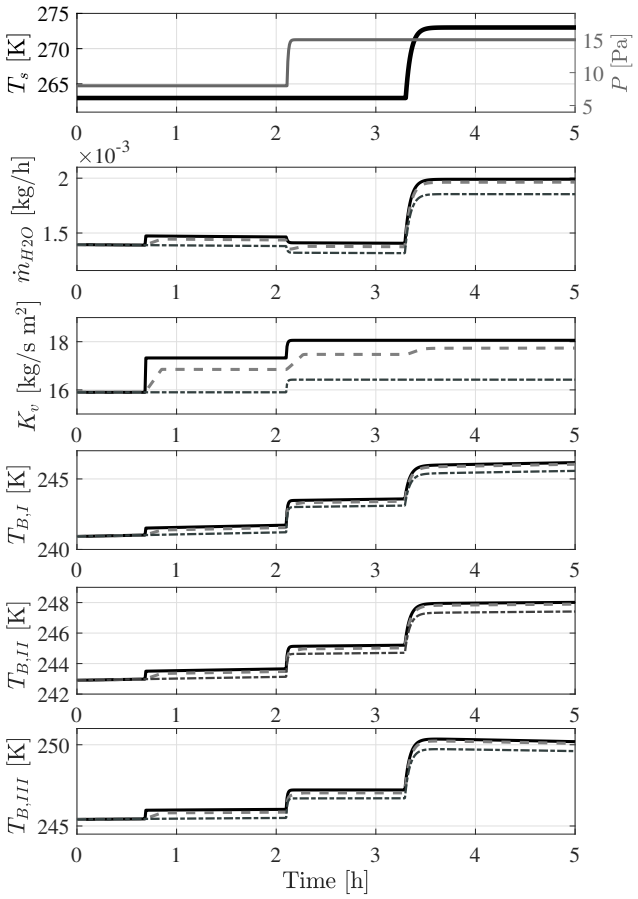

Fig. 4. Estimation results scenario 1 (parametric disturbances). Simulated process (—), results from proposed estimator (– –) and open-loop observer (–•).

scenario. It comprises the process representation (phenomenological model) inputted with T_s and P, and the nominal values of the heat transfer coefficient, providing the output predictions without measurement feedback. The difference between the estimated and process values results in the estimation error. The performance benchmarks are based on the root mean square error (RMSE) of the estimation.

Figure 4 presents the results of the first simulation scenario. In this cycle, parametric disturbances are included in the nominal K_v of the plant, indicating errors in the *apriori* calibration of the coefficients that relate K_v to the chamber pressure and the vial geometry. For that purpose, k_2 and k_3 in (6) are purposely biased by a multiplying factor to create a mismatch of 30% between model and process starting at 0.7 h and thereafter.

Due to the mismatch after 0.7 h, the open-loop results underestimate the predicted product temperature by up to 0.6 K, and the resulting global flow rate of water vapor $\hat{m}_{\mathrm{H_2O}}$. In the proposed estimator, the discrepancy in product temperature is reduced to 0.1 K. Note that Λ is set to 0.4, to penalize the difference between nominal K_v and their estimate, and after the disturbance is introduced, $\hat{K}_v$ varies to approach the estimated $\dot{m}_{\mathrm{H_2O}}$ to the measured value, but it does not overlap it. Λ acts as a tuning weight and expresses the confidence level on the prior calibration

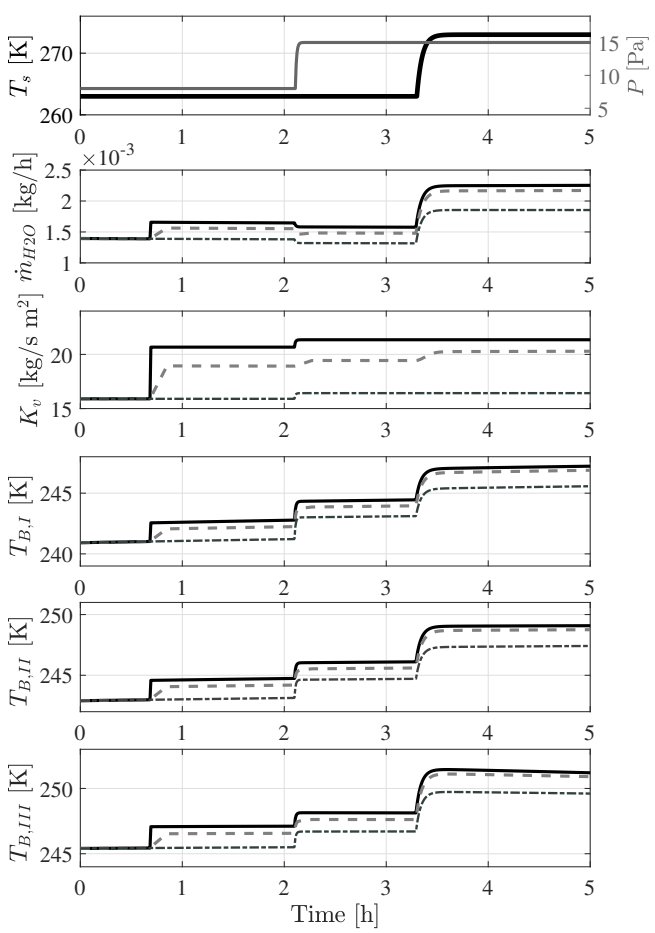

Fig. 5. Estimation results scenario 2 (parametric disturbances, measurement noise, and biased readings). Simulated process (—), results from proposed estimator (– –) and open-loop observer (–·).

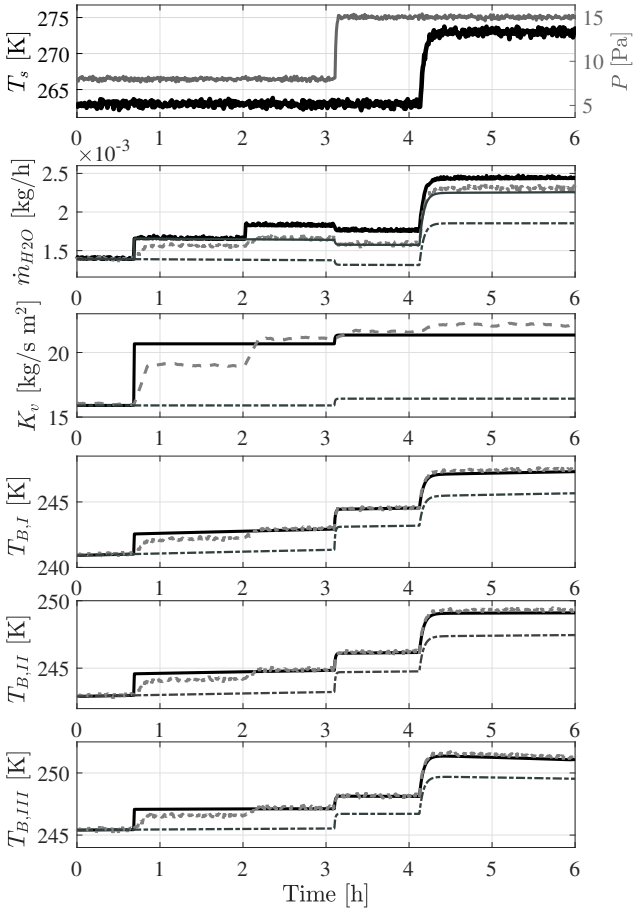

Fig. 6. Estimation results scenario 3 (parametric disturbances, measurement noise, and biased readings). Simulated process with measurement noise and bias (—), $\dot{m}_{\mathrm{H_2O}}$ without measurement errors (—), results from proposed estimator (– –) and open-loop observer (–·).

of the heat transfer coefficient. The estimation window in (10) is $\mathcal{N} = 20$ samples, considering the sampling time of $\Delta t = 30$ s. The longer the estimation window, the slower the convergence will be in the face of disturbances.

In the second scenario, illustrated in Figure 5, the mismatch between plant and model is enlarged by including an additional 30% in k_1 of the plant, that is, the calibrated parameter that relates K_v with the vial position in the chamber. In the presence of a larger mismatch, the difference in the predicted product temperature in the open-loop goes up to 1.6 K, which results in a drying time 15% longer than the one in the process. In the proposed estimator, the deviation in product temperature is reduced to 0.5 K, and the predicted drying time is only 4.9% longer than the one in the process.

The third scenario, presented in Figure 6, evaluates the estimator in the presence of parametric disturbances, measurement noise, and biased sensor readings. Apart from the plant/model mismatch in K_v at 0.7 h, white Gaussian noise is included in each measured variable, and a step disturbance is applied to $\dot{m}_{\mathrm{H_2O}}$ at 2.1 h with an amplitude of $0.2\ \mathrm{E}-3$ kg h^{-1}. In practice, the instrumentation used for the chamber pressure and shelf temperature provides accurate readings, and only noise in the sensor signal is expected. However, the measurement of the global flow rate of water vapor is typically an indirect reading and may be subject to noise and bias.

For the open-loop estimator, the bias in $\hat{\dot{m}}_{\mathrm{H_2O}}$ has no impact. However, the parametric disturbances result in underestimated predictions of T_B by more than 1.7 K. The input noise is reflected in the predictions of T_B of the proposed estimator. At 2.1 h, the insertion of the step bias in the measured $\dot{m}_{\mathrm{H_2O}}$ results in an overestimation of around 0.3 K in the product temperature of each vial. The weight that penalizes the deviation from the nominal K_v, Λ, protects the prediction from drifting too far from the unbiased value of $\dot{m}_{\mathrm{H_2O}}$. This parameter is part of the experimental design and could be adjusted based on the confidence level between the calibrated K_v and the experimental measurement. Table 3 summarizes the estimator performance regarding the RMSE of K_v, $\dot{m}_{\mathrm{H_2O}}$, and the product temperatures of vials in zone I $T_{B,I}$.

The proposed estimator exhibits a better performance overall under parametric disturbances and model mismatches. These results validate in simulation the possibility of estimating the product temperature of multiple

Table 3. RMSE of the estimations of $T_{B,I}$, $\dot{m}_{\mathrm{H_2O}}$, and K_v in each simulation case.

Scenario	Open-loop			Estimator		
	K_v [J/m^{2}s K]	$\dot{m}_{\mathrm{H_2O}}$ [kg/h]	$T_{B,I}$ [K]	K_v [J/m^{2}s K]	$\dot{m}_{\mathrm{H_2O}}$ [kg/h]	$T_{B,I}$ [K]
1	1.46	1E − 4	0.49	1.67	0.3E−4	0.14
2	4.55	3E − 4	1.43	1.28	0.9E−4	0.44
2	4.55	3E − 4	1.46	1.28	0.6E−4	0.32

vials, and total cycle time using the measurement of the sublimation flow rate of water vapor and calibrated models.

5. CONCLUSIONS

The objective of this paper was to introduce an estimator for the multi-vial process of primary drying using a global measurement of the flow rate of sublimed water vapor. The benefits of the proposed approach were illustrated using a case study of a previously characterized product. Results allow comparing the quality of the estimates with respect to product temperature under parametric disturbances, plant/model mismatch, measurement noise, and a biased measurement of $\dot{m}_{\mathrm{H_2O}}$. An open-loop estimator containing the phenomenological model calibrated with nominal parameters provided the baseline for performance comparison. The results show that the proposed approach provides better estimates of T_B than the open-loop case when faced with parametric disturbances. The estimated product temperature bias could also result in an additional 15% of cycle time for this case study. Considering the careful selection of appropriate instrumentation, this work opens the possibility of using a non-invasive measurement of sublimed water vapor to predict the key variables of multi-vial primary drying.

ACKNOWLEDGEMENTS

The authors acknowledge the financial support of MITACS and Pfizer.

REFERENCES

Barresi, A.A., Pisano, R., Rasetto, V., Fissore, D., and Marchisio, D.L. (2010). Model-based monitoring and control of industrial freeze-drying processes: effect of batch nonuniformity. *Drying Technology*, 28(5), 577–590.

Bosca, S., Barresi, A.A., and Fissore, D. (2017). On the robustness of the soft sensors used to monitor a vial freeze-drying process. *Drying Technology*, 35(9), 1085–1097.

Chia, A., Bouchard, J., Ratti, C., and Poulin, É. (2022). Development and calibration of a lyophilization model for process control applications. *22 International Drying Symposium*.

Chia, A., Poulin, É., Bouchard, J., Lapointe-Garant, P.P., Van Meervenne, B., and Taveirne, F. (2023). Experimental validation of multi-vial control for primary drying in a pilot-scale unit. *Chemical Engineering Research and Design*, 193, 281–293.

Fissore, D., Pisano, R., and Barresi, A.A. (2010). On the methods based on the pressure rise test for monitoring a freeze-drying process. *Drying Technology*, 29(1), 73–90.

Fissore, D., Pisano, R., and Barresi, A.A. (2015). Method for monitoring primary drying of a freeze-drying process. US Patent 9,170,049.

Fissore, D., Pisano, R., and Barresi, A.A. (2017). On the use of temperature measurement to monitor a freeze-drying process for pharmaceuticals. In *Instrumentation and Measurement Technology Conference (I2MTC), 2017 IEEE International*, 1–6. IEEE.

Pikal, M.J. (1985). Use of laboratory data in freeze drying process design: heat and mass transfer coefficients and the computer simulation of freeze drying. *PDA Journal of Pharmaceutical Science and Technology*, 39(3), 115–139.

Pikal, M.J. (2000). Heat and mass transfer in low pressure gases: applications to freeze drying. *Drugs and the Pharmaceutical Sciences*, 102, 611–686.

Pikal, M.J., Bogner, R., Mudhivarthi, V., Sharma, P., and Sane, P. (2016). Freeze-drying process development and scale-up: scale-up of edge vial versus center vial heat transfer coefficients, kv. *Journal of pharmaceutical sciences*, 105(11), 3333–3343.

Pikal, M.J., Roy, M., and Shah, S. (1984). Mass and heat transfer in vial freeze-drying of pharmaceuticals: Role of the vial. *Journal of pharmaceutical sciences*, 73(9), 1224–1237.

Pisano, R., Ferri, G., Fissore, D., and Barresi, A.A. (2017). Freeze-drying monitoring via pressure rise test: The role of the pressure sensor dynamics. In *2017 IEEE International Instrumentation and Measurement Technology Conference (I2MTC)*, 1–6. IEEE.

Pisano, R., Fissore, D., and Barresi, A.A. (2014). A new method based on the regression of step response data for monitoring a freeze-drying cycle. *Journal of Pharmaceutical Sciences*, 103(6), 1756–1765.

Pisano, R., Fissore, D., and Barresi, A.A. (2016). Non-invasive monitoring of a freeze-drying process for tert-butanol/water cosolvent-based formulations. *Industrial & Engineering Chemistry Research*, 55(19), 5670–5680.

Rajniak, P., Moreira, J., Tsinontides, S., Pham, D., and Bermingham, S. (2022). Integrated use of mechanistic models and targeted experiments for development, scale-up and optimization of lyophilization cycles: A single vial approach for primary drying. *Drying Technology*, 40(2), 310–325.

Sharma, P., Kessler, W.J., Bogner, R., Thakur, M., and Pikal, M.J. (2019). Applications of the tunable diode laser absorption spectroscopy: in-process estimation of primary drying heterogeneity and product temperature during lyophilization. *Journal of pharmaceutical sciences*, 108(1), 416–430.

Stratta, L., Capozzi, L.C., Franzino, S., and Pisano, R. (2020). Economic analysis of a freeze-drying cycle. *Processes*, 8(11), 1399.

Velardi, S.A., Hammouri, H., and Barresi, A.A. (2009). In-line monitoring of the primary drying phase of the freeze-drying process in vial by means of a kalman filter based observer. *Chemical Engineering Research and Design*, 87(10), 1409–1419.

Velardi, S.A., Hammouri, H., and Barresi, A.A. (2010). Development of a high gain observer for in-line monitoring of sublimation in vial freeze drying. *Drying Technology*, 28(2), 256–268.